

SPECIAL ISSUE: CELEBRATING 20 YEARS OF GEOGRAPHY IN KADUNA STATE UNIVERSITY - ADVANCES AND FRONTIERS IN GEOGRAPHY

Examining the Relationship between Green Space Depletion and the Urban Heat Island Effect in Sokoto Metropolis, Sokoto State, Nigeria

Abdullahi Umar  ^a, Aminatu Kabir Ibrahim  ^b, Kabiru Bilal  ^b, Habibu Musa Gebbe  ^b, Kabir Sulaiman  ^b

^a Department of Geography, Federal University, Birnin Kebbi, Kebbi State, Nigeria ^b Department of Environmental and Resources Management, Usmanu Danfodiyo University, Sokoto, Nigeria

ABSTRACT

This study examined green space depletion (GSD) and its relationship with the urban heat island (UHI) effect in Sokoto metropolis, Nigeria. Landsat TM, ETM+, and OLI/TIRS bands and land surface temperature (LST) data for the periods 2000, 2015, and 2025 were obtained from the USGS Earth Explorer. The images were analysed, where land surface temperature (LST) extent, and normalized difference vegetation index (NDVI) were generated. Analysis of NDVI maps for the period indicates a consistent decline in vegetation cover, where vegetated areas decreased from approximately 42% in 2000 to 32% in 2015 and further to approximately 20% in 2025. This represents a total vegetation loss of more than 50% over 25 years across the metropolis. Findings reveal that the city experienced a nearly 100% increase in high-temperature surface coverage within 25 years, confirming a rapidly intensifying UHI effect. There is a significant negative correlation between the LST and NDVI, indicating that low NDVI values tend to have relatively high LST values, contributing to the formation of UHI hotspots. Central, southern, and western areas (Mabera, Kasarawa, Runjin Sambo, and Guiwa low-cost/Guiwa village) exhibited high UHI intensity. These areas happened to get minimal green spaces. The study concludes that there is spatial concurrence of GSD and UHI hotspots. This manifested in a clear spatial association between areas of GSD and UHI hotspots; impervious, densely built areas that exhibit higher LSTs. This study recommends robust re-greening efforts and the safeguarding of green spaces in the Sokoto metropolis to mitigate the UHI effect.

ARTICLE HISTORY

Submitted 24 October 2025
Accepted 20 December 2025
Published 21 December 2025

GUEST EDITOR

A. M. Ahmed

KEYWORDS

Green Space Depletion;
Urban Heat Island, NDVI;
Land Surface Temperature;
Urban Hotspots; Sokoto
Metropolis

1 Introduction

Urbanization, especially in developing countries such as Nigeria, is a rapidly accelerating phenomenon. It leads to the transformation of urban landscapes through drastic changes and grey space's takeover of green spaces in cities where land cover is limited not only to urban parks and gardens but also to unsealed, permeable, "soft" surfaces such as soil, grass, shrubs and trees, which are privately or publicly accessible or managed (Umar et al., 2018; Mensah, 2014). It has been acknowledged that tampering with urban components has considerable consequences, sometimes even unwanted repercussions on other elements, which subsequently affect the welfare and well-being of inhabitants (Umar et al., 2018). One such unwanted repercussion on urban natural landscapes arising from green space depletion and environmental problems is the urban heat island (UHI) effect, which makes cities hotter and less comfortable than other areas as a result of the exacerbation of thermal physiological discomfort (Murtinová et al., 2022). Increased temperatures in urban areas can worsen heat-related health problems, increase energy demand for cooling, and reduce overall quality of life (Zhou et al., 2017).

It has been asserted that urban areas need to be made

harmonious with nature, with full consideration and respect for their ecological, cultural, and religious heritage and the diversity of the environment, if environmental sustainability is to be achieved. The UHI effect occurs when urban areas experience higher temperatures than surrounding rural areas due to human activities and changes in land use/land cover (LULC). This temperature discrepancy is driven by the major factors of the replacement of natural land cover with impervious surfaces such as concrete, asphalt, and buildings, which are very good heat absorbers and retainers (Yan et al., 2023). Green spaces play a crucial role in mitigating the UHI effect by providing shade, facilitating evapotranspiration, and enhancing urban albedo. However, rapid urban expansion and sprawl, especially in low-income and poorly planned urban centers, often lead to the depletion of these green spaces. This depletion has implications for the local climate, particularly with respect to the UHI effect.

An NDVI analysis of satellite images and green belt maps of the study area by Eniolorunda and Dankani (2020) for a time span of seventeen years (from 1998 to 2015) revealed that the study area was greener in 1998 (with approximately 1,108ha vegetated) than in 2015,

when it was only 543 ha, representing 36.1% and 17.7% of the total area, respectively.

Studies (such as Umar et al., 2018; Yelwa et al., 2009; Eniolorunda, 2010; Adamu et al., 2015; Adamu & Umar, 2015) have documented the emergence of ecological faults and offences as in flagrant residential encroachment into the adjoining agricultural Sokoto-Rima floodplain, and the degradation of the greenbelts, which combine to have implications for individuals' coping with thermal discomfort in the city.

This research improves upon these studies through the examination and analysis of GSD and its relationship with the UHI effect via GIS and remote sensing techniques. The aim of this research is therefore to examine the relationship between green space depletion and the urban heat island effect in the Sokoto metropolis. The objectives set for the study were to identify urban heat island hotspots, determine the relationship between green space loss and UHI intensity, and examine temporal changes in LST and NDVI in the study area.

2 Materials and Methods

2.1 Study Area

The Sokoto Metropolis is located in an area between longitudes 5.136040° E to 5.302310° E and latitudes 12.956610° N to 13.083790° N, which is located in the dryland region of northwestern Nigeria. The climate of the area is characterized by high temperatures (as high as 43°C around March/April, which is during the hot dry season), low annual rainfall, and sparse vegetation. The climate of the area is tropical wet and dry and is coded *Aw* by Köppen's classification, and is characterized by

high variability in temperature, rainfall, and humidity. Between March and May, during the hot-dry season, the weather is hot and dry, and less than 1% of the annual rainfall (mango rain) is experienced and recorded in May. Rainfall is experienced in the study areas when warm, moist tropical maritime (South Westerly) air masses and hot and dry tropical continental (North Easterly) air masses interact (Umar et al., 2018). The two air masses meet along the inter-tropical convergence zone (ITCZ), which moves in response to the seasonal disposition of the overhead sun. Rainfall amounts are generally related to the thickness of the Tropical Maritime air mass. The annual rainfall is approximately 600 mm, while mean annual minimum and maximum temperatures of 21.50 °C and 34.90 °C, respectively, have been recorded (Umar et al., 2018; Umar, 2013). The dry season spans November to April (Eniolorunda & Dankani, 2020).

The metropolis covers a roughly circular area that extends to a 16 km radius that entails four local government areas (LGAs), namely, Sokoto North, Sokoto South, Wamakko, and part of Kware LGAs (Umar et al., 2018; Dantuni, 2011). On the basis of the 2006 population census, the metropolitan area has been projected to have a population of approximately 503,256 people by 2015, with a population density of 95.9 persons per square kilometer and a 3% annual growth rate (NPC, 2007). The Sokoto metropolis, Nigeria, is characterized by arid climatic conditions, rapid urban development, and the consequent depletion of green infrastructure; thus, it has become a significant environmental issue that warrants examination.

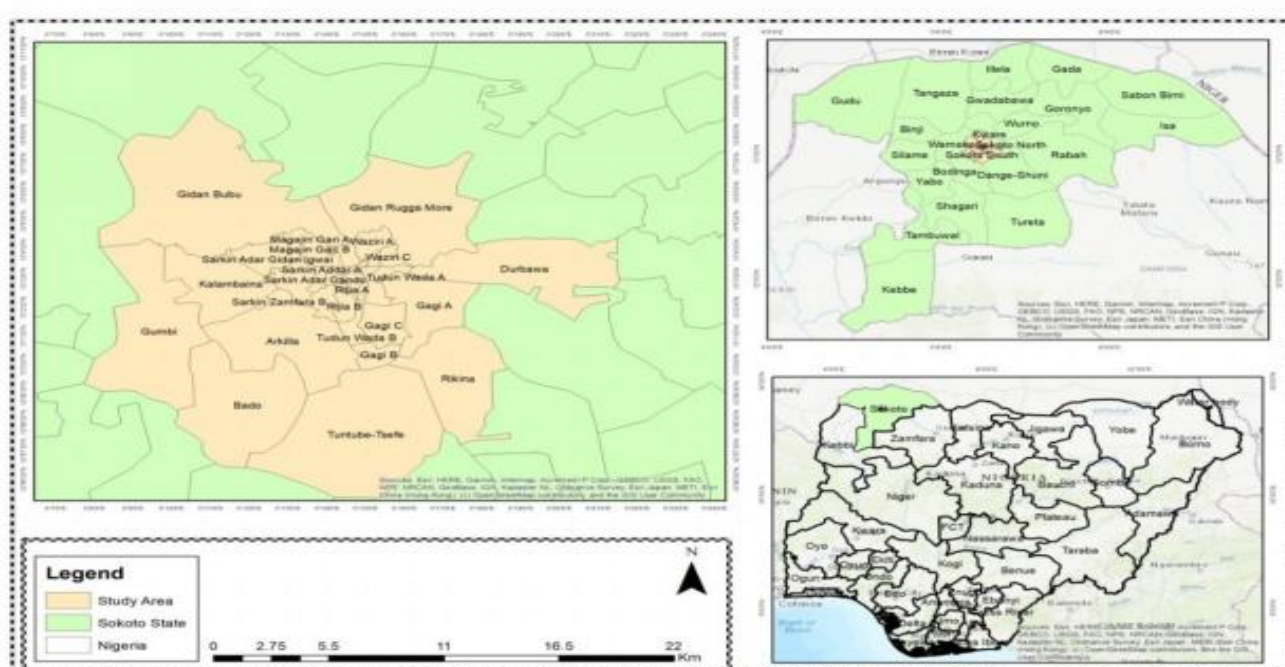


Figure 1: Sokoto Metropolis

Source: Sokoto State Geographic Information System Agency, 2025



2.2 Data Sources

Landsat TM, ETM+, and OLITIR bands for the periods April 2000, 2015, and 2025 were downloaded from the USGS Earth Explorer (or derived from Landsat thermal bands). Landsat satellite images (2000–2025) were analysed, where the land surface temperature (LST) extent, an index used to measure UHIs, and the normalized difference vegetation index (NDVI), an index used to establish a relationship between green space loss and UHI intensity, were generated.

The satellite imagery used in the study, as shown in Table 1, is Landsat (TM/ETM+/OLI/TIRS). This method

has been used for vegetation indices. The images consisted of time series ranging from 2000–2025. Thermal bands (Landsat 7 & 8 TIR) were used for LST retrieval. The images obtained were Cloud-free for the dry season. Ancillary maps were generated from administrative boundary shapefiles, road networks, and land parcel maps from local authorities in the GIS environment. The GIS and remote sensing tools and software used for statistical analysis and visualization were ArcGIS 10.5.

Table 1: Data used and sources

Data Type	Source	Time frame	Purpose
Landsat TM, ETM+, OLITIR bands	USGS Earth Explorer	April 2000, 2015, 2025	LST extraction
Land Surface Temperature (LST)	Derived from thermal bands of Landsat	April 2000, 2015, 2025	To estimate Urban Heat Island intensity
NDVI and vegetation indices	Calculated from Landsat multispectral bands	April 2000, 2015, 2025	To measure green space coverage and vegetation health
Administrative boundary maps	OSM, National Population Commission (NPC)	Latest available	For clipping and geo-referencing

2.3 Data Collection

As explained in section 2.2.1, the images (Landsat TM, ETM+, and OLITIR bands) for the target years were downloaded from the USGS Earth Explorer (Landsat). The land surface temperature (LST) was derived from the thermal bands of Landsat to estimate the urban heat island intensity. Table 2 shows that all the images were acquired during the dry season when the cloud cover was minimal at less than 10%; as such, they were cloud-free. This implies better data retention after masking and improved classification, radiometric, and atmospheric correction accuracies.

Table 2: Specification of the images used

S/N	Years	Acquisition Date	Sensor Type	Path/Row	Metadata	Spatial Resolution (m)	Cloud Cover
1	2000	2000-04-26	Landsat 7	191/051	Band 3, 4, and 6.	30	< 10
2	2015	2015-04-28	Landsat 8	191/051	Band 4, 5, and 10.	30	< 10
3	2025	2025-04-07	Landsat 8	191/051	Band 4, 5, and 10.	30	< 10

2.4 Data Analysis

Radiometric Pre-processing of Satellite Imagery (RPSI)

During the RPSI multispectral band processing, the three normal stages were followed. These are the digital number (DN), spectral radiance, and top-of-atmosphere (TOA) reflectance. This process yielded the generation

and retrieval of the following:

Vegetation indices

An NDVI spectral index was computed where the spatial distribution was mapped, and zonal statistics were calculated (mean NDVI per administrative unit).

Land Surface Temperature (LST) Retrieval

In the process of estimating the actual ground surface temperature from thermal infrared bands (Landsat 8), the following standard steps were followed:

- i. The thermal band DN was converted to spectral radiance.
- ii. The spectral radiance was converted to the at-sensor brightness temperature (in Kelvin) via sensor-specific constants.
- iii. The surface emissivity was corrected via the normalized difference vegetation index (NDVI) threshold method to estimate emissivity from the vegetation proportion.
- iv. Emissivity correction was applied to obtain the LST at °C.
- v. The land surface temperature was calculated via Eqn. (1):

$$LST = \left(\frac{BT}{1 + \left(\lambda * \frac{BT}{\rho} \right) * \ln(\epsilon)} \right) - 273.15 \quad (1)$$

Where:

BT - At-sensor brightness temperature

λ - Wavelength of emitted radiance

$\rho = h * c / s$ (1.438 × 10⁻² m K) or 14,380

h - Planck's constant (6.626 × 10⁻³⁴ Js)

s - Boltzmann constant (1.38 × 10⁻²³ J/K)

c - Velocity of light (2.998 × 10⁸ m/s)

ϵ - Emissivity

To obtain the LST using Eq. (1), the effective at-satellite temperatures of the viewed Earth-atmosphere system are a physically useful variable. It can be obtained when the spectral radiance of the thermal bands TM and ETM++ under the assumption of unity emissivity is converted using Eqn. (2):

$$BT = \frac{K2}{(K1 + 1)} \quad (2)$$

Where:

BT - Effective at-satellite temperature in Kelvin

K1 - Calibration constant 1 (W/(cm² * sr * μm))

K2 - Calibration constant 2 (K)

L λ - Spectral radiance (Watts/(m² * sr * μm))

DN Conversion to TOA reflectance

The quantity of solar radiation reflected by the Earth's surface and calculated by the satellite sensors is tailored by its interface with the atmosphere. The raw digital

numbers are not reflective of the true surface reflectance values. Therefore, atmospheric correction is required to bring the image to top of atmosphere (TOA) radiance, by removing atmospheric effects from satellite images (Abdelnour & Engel, 2018; Hadjimitsis & Themistocleous, 2008). To get the useful at-sensor brightness temperature, radiometric corrections were conducted to acquire TOA radiances. Initially, the digital numbers were transformed to spectral radiance using Eqn. (3):

$$L\lambda = \left(\frac{LMAX\lambda - LMIN\lambda}{QCALMAX - QCALMIN} \right) * (QCAL - QCALMIN) + LMIN \quad (3)$$

Where:

$L\lambda$ - Spectral radiance at the sensor's aperture (Watts/(m² * sr * μm))

QCAL - Quantized calibrated pixel value in DN

$LMIN\lambda$ - Spectral radiance scaled to QCALMIN (Watts/(m² * sr * μm))

$LMAX\lambda$ - Spectral radiance scaled to QCALMAX (Watts/(m² * sr * μm))

QCALMIN - Minimum quantized calibrated pixel value (corresponding to $LMIN\lambda$) in DN

QCALMAX - Maximum quantized calibrated pixel value (corresponding to $LMAX\lambda$) in DN

For Landsat TIRS, equation 4 was used to bring the thermal band (Bands 10) to TOA radiance:

$$L\lambda = M_L Q_{cal} + A_L \quad (4)$$

Where: M_L - Band-specific multiplicative rescaling factor

A_L - Band-specific additive rescaling factor

Q_{cal} - Quantized and calibrated standard product pixel values (DN)

Land surface emissivity (LSE)

Surface emissivity is the ability of the surface to convert heat energy into quantifiable radiant energy. Retrieval of LST is entirely dependent upon the ability of the land surface to convert heat energy into radiant energy. The emissivity (ϵ) was ascertained using equation 5.

$$\epsilon = 0.004 Pv + 0.986 \quad (5)$$

Where: Pv is the proportional vegetation given by

$$\frac{NDVI - NDVI_{min}}{NDVI_{max} - NDVI_{min}}^2$$

UHI Mapping and Metrics

The difference between the urban core mean LST and the rural/peri-urban mean LST was computed (UHI

intensity). Maps of LST were produced and classified into temperature zones (e.g., low, moderate, and high) to visualize UHI hotspots. A spatial overlay was used to compare the LST maps with the NDVI maps to identify spatial correspondence between low vegetation and high LST.

Statistical analysis

Descriptive statistics (mean and standard deviation) for the LST and NDVI were computed. Also, relationships between vegetation metrics (NDVI) and LST were tested via Pearson correlation coefficients. All five assumptions of Pearson's correlation (r), namely: linearity, data level of measurement, normality, homoscedasticity, and independence of observations, were met. The LST-NDVI coefficients, emanating from dense urban area shows an inverse relationship which is not strictly (but approximately) linear, and Pearson is interested or measures only the strength of linear association. Secondly, the level of measurement of LST (in Kelvin) and NDVI (an index ranging from -1 to +1) are both continuous (interval/ratio data). The two variables (LST and NDVI) are approximately normally distributed. With regards to homoscedasticity, Table 4 shows that the standard deviations (variance) of the two variables are similar (all progressing from the year 2000 to 2025). Lastly, the LST and NDVI pixels are independent (spatially autocorrelated).

2.5 Data Analysis

The data were cleaned, coded, and analyzed using descriptive statistics, including frequencies and

percentages. In addition, cross-tabulation was applied as the primary analytical technique to compare responses across wards, gender, age groups, education levels, and occupations. This method allowed for deeper spatial and socio-demographic interpretation of community participation patterns, governance effectiveness, and barriers to engagement in Chikun LGA. All results were presented in cross-tabulated tables to enhance clarity and support detailed comparison.

3 Results

3.1 Spatial distribution and patterns of UHI hotspots

To identify and map urban heat island (UHI) hotspots in relation to green space depletion in the study area, this study used geospatial analysis and generated the land surface temperature (LST) and normalized difference vegetation index (NDVI). Sections 3.1.1 and 3.1.2 present the spatial distribution and patterns of land surface temperature (LST), an index used to measure UHIs, and the normalized difference vegetation index (NDVI), an index used to establish the relationship between green space loss and UHI intensity, were generated.

3.2 Land Surface Temperature Extent

Figure 2 shows the spatial distributions of land surface temperature (LST) across Sokoto Metropolis for 2000, 2015, and 2025. The maps were derived from Landsat thermal bands and classified into three temperature categories, i.e., low, moderate, and high, to visualize spatial variations in surface heat intensity.

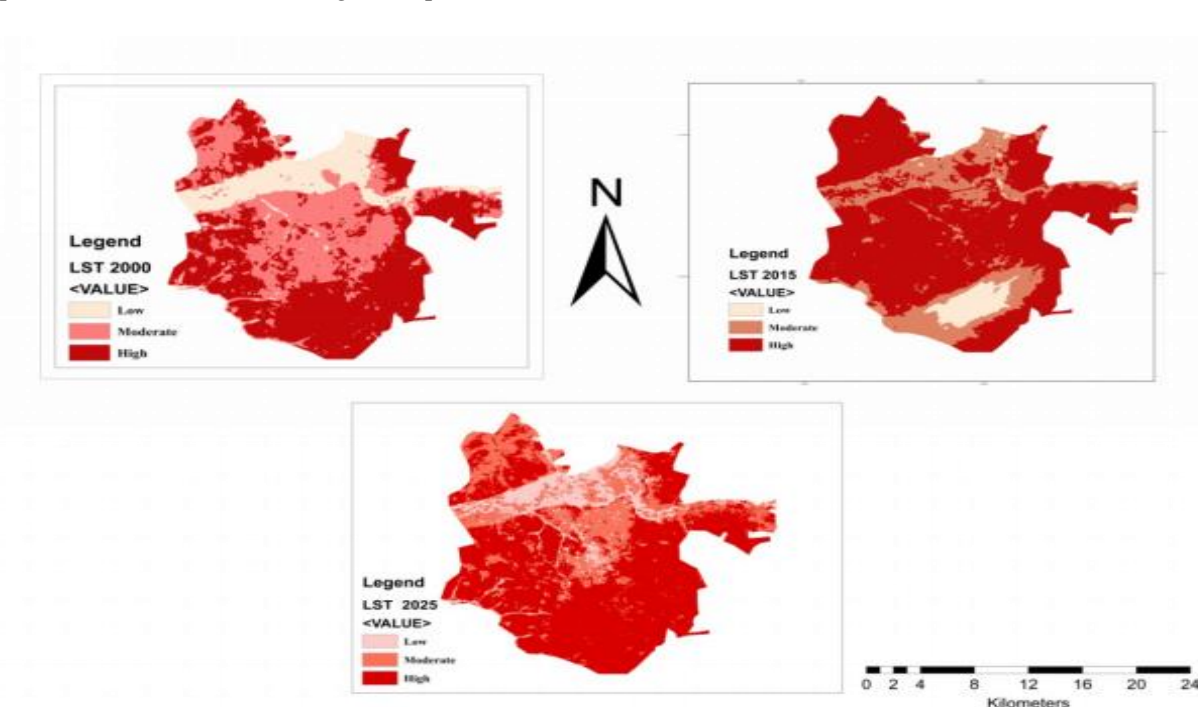


Figure 2: Land surface temperature (LST) extent map from 2000-2025

In 2000, low-LST areas were visible mainly in the central-northern and northeastern parts of the metropolis. These are areas within and adjacent to the Sokoto-Rima River flood plains with more vegetation, agricultural lands, or bare moist surfaces (see Figure 3). Moderate LST areas form transitional bands around cooler zones (areas around Gidan Iwai, Runjin Sambo, Gandu, etc.). High-LST zones dominate the southern half of the metropolis

and parts of the western and south-eastern regions (around Gwiwa village, Gwiwa Low Cost, Bafarawa Estate, Old Airport, Salame, etc.). These zones correspond to dense bare soil, rocky surfaces, or early-developing built-up regions and sparsely vegetated areas that absorb and retain more heat. The heat distribution is mixed, with approximately 40–50% high-temperature coverage.

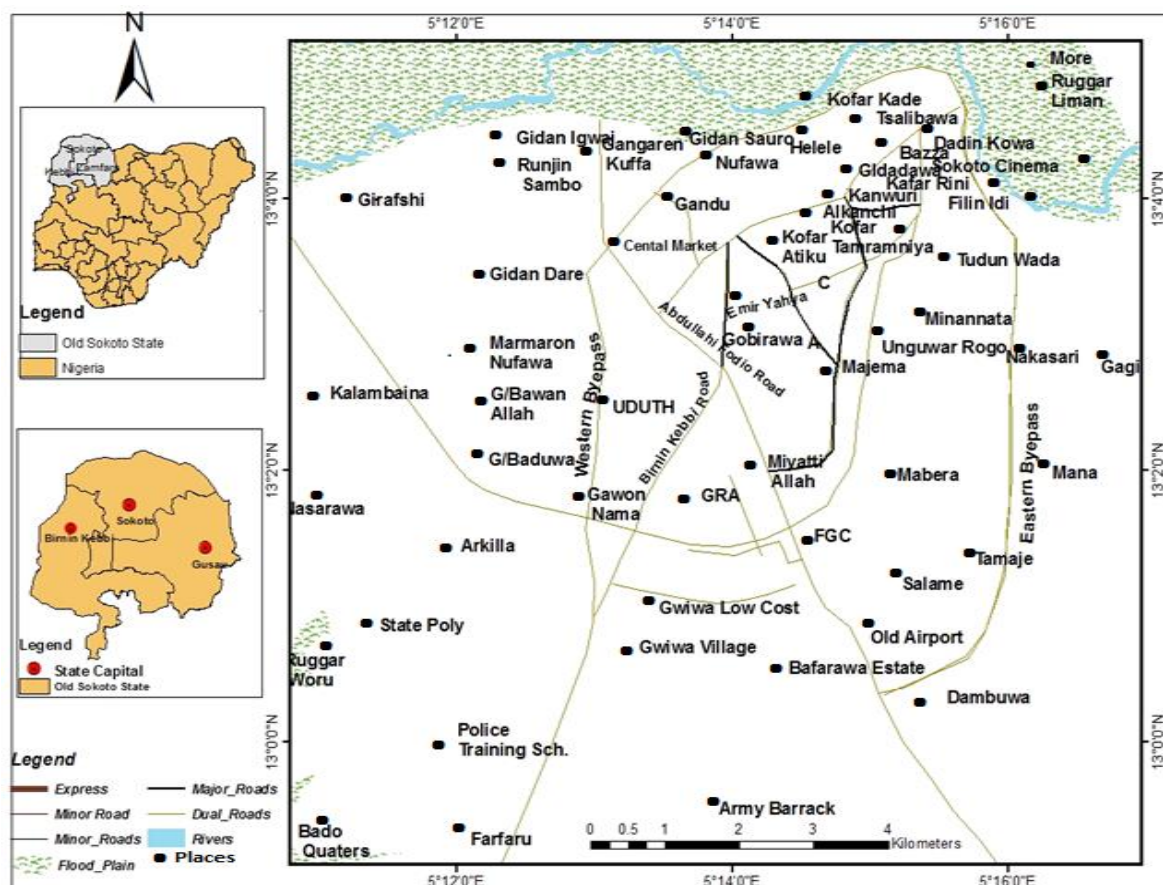


Figure 3: Location map of the areas of the Sokoto metropolis

By 2015, high-temperature zones had expanded significantly. The low-temperature zones shrink dramatically and are limited to small pockets in the far northeast and south-central areas, implying a loss of surface cooling potential due to vegetation reduction, a decline in natural vegetation, and an increase in built-up surfaces. Moderate-LST zones thin out and begin to merge with high-LST zones. High-LST areas become dominant across almost the entire central metropolis, large parts of the west, nearly all of the south, and much of the east. This increase in surface temperature can be attributed to rapid urban expansion and reduced surface cooling, likely driven by the replacement of vegetated areas with impervious surfaces and a reduction in evapotranspiration. High-temperature zones cover approximately 65–75% of the metropolis. This indicates a noticeable warming trend and matches the NDVI vegetation loss between 2000 and 2015.

By 2025, the entire surface of the metropolis is almost uniformly hot. Low-LST zones become extremely scarce, and only tiny patches remain. The moderate-LST regions are now thin, with scattered strips occurring mainly in the northern corridor. High-LST areas constitute 80–90%+ of the metropolis area. The LST maps for 2000, 2015, and 2025 clearly reveal the intensification of surface temperatures in Sokoto Metropolis. High-temperature zones expanded from approximately 45% in 2000 to over 70% in 2015 and further to more than 85% by 2025. The low-temperature areas nearly disappeared. The spatial pattern reveals that warming is strongest in the central, southern, western, and eastern parts of the metropolis, which coincides with areas experiencing the most vegetation loss and urban expansion. Overall, the Sokoto city shows a nearly 100% increase in high-temperature surface coverage within 25 years, confirming a rapidly intensifying urban heat island effect.



3.3 Vegetation Cover Distribution (NDVI)

Figure 4 presents the NDVI-based vegetation cover maps for 2000, 2015, and 2025. The NDVI classification distinguishes between vegetated areas (green zones) and non-vegetated areas (beige zones), reflecting the extent and spatial distribution of green cover in the study area. A number of studies have also shown that the NDVI values of river banks and around water bodies are higher

than those of other classes. There was a remarkable decrease in tree density in the eastern, northwestern, and western parts of the city. This signifies a profound effect of urbanization pressure on urban vegetation, which may lead to the degradation or loss of native tree species through initial habitat transformation or landscape fragmentation processes as urban areas expand, corroborating the findings of Dangulla et al. (2024).

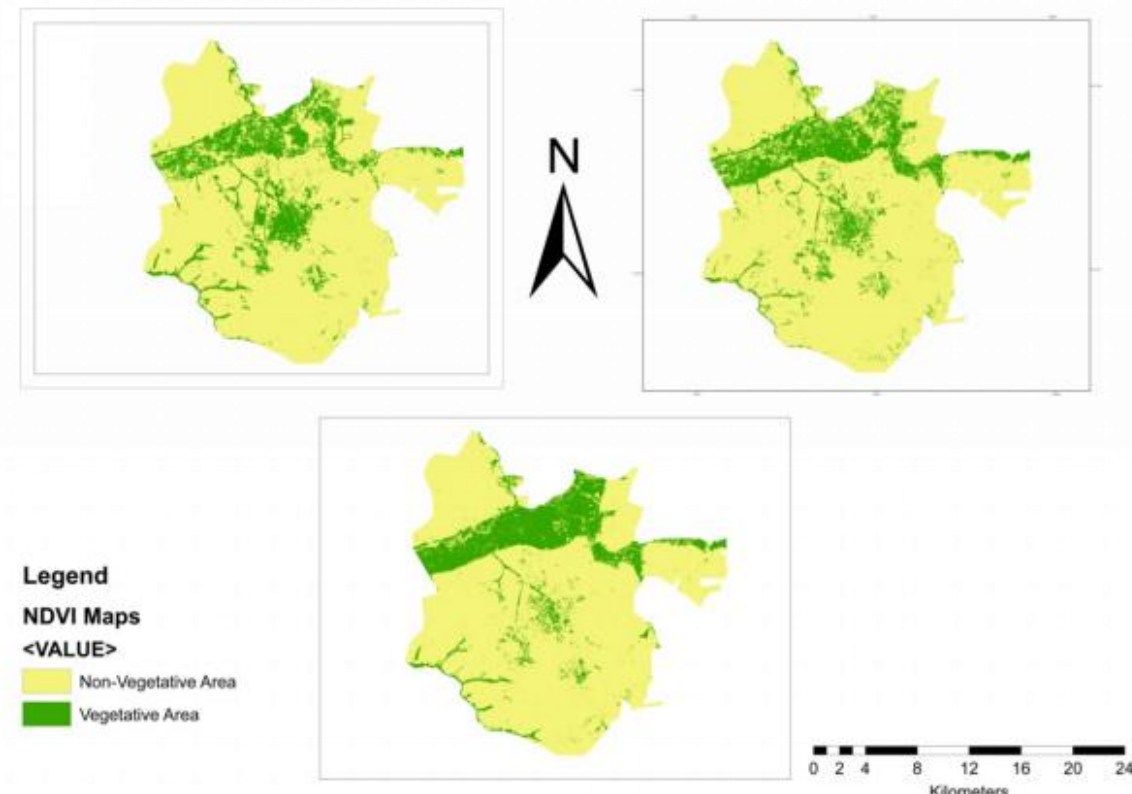


Figure 4: Vegetation cover of Sokoto metropolis in 2000, 2015, and 2025

In 2000, vegetation was relatively abundant and widespread, particularly in the northern, central, and eastern regions of the Sokoto metropolis. This suggests a lower degree of urban development at that time, with the presence of natural vegetation, along agricultural belts, river corridors, and peri-urban zones, and open green spaces contributing to the ecological balance and lower surface temperatures. By 2015, vegetation cover had become sparse and highly discontinuous, and only scattered patches remained, mostly along waterways and isolated agricultural pockets. There was a notable decline in vegetated areas, especially within the central and western parts of the city. The expansion of built-up and non-vegetated surfaces is evident, indicating deforestation, land conversion, and increased urban encroachment. This reduction in vegetation cover directly correlates with the observed increase in LST, confirming the inverse relationship between vegetation density and surface temperature. The losses were more visible in the

central parts as the metropolis expanded outwards.

By 2025, the vegetation in Sokoto Metropolis is fragmented and unevenly distributed. The vegetation cover becomes sparse and highly discontinuous. Only scattered patches remained concentrated around riverbanks and agricultural patches. There was a remarkable decrease in vegetation cover dominating the southern and western zones, indicating urban expansion, bare land, or dry regions. The majority of the area appears non-vegetative, likely due to urbanization, arid conditions, and limited green cover. This pattern reflects climatic stress and land-use changes over time (e.g., spontaneous urban growth).

3.4 Identification of UHI Hotspots

Hotspot analysis showed progressive changes; in 2000, hotspots were isolated, mainly in the south-west. By 2015, hotspots became larger and more dispersed across central and southern sectors (see figure 5). Hotspots formed continuous belts in the south, south-west, and south-east.

These spatial patterns strongly correlate with urban expansion and declining vegetation cover. The 2000 hotspot map shows few, isolated, and small hotspots, concentrated mainly in the south-western portions of the metropolis. Most other areas displayed low thermal clustering. This suggests early-stage urban development and minimal UHI formation. Low hotspot intensity is typical of cities with significant natural land cover and low population density (Kong et al., 2021).

By 2015, hotspots became more numerous and spatially dispersed, extending into central and southern

regions. Patches were larger and more fragmented than in 2000. This reflects accelerated urbanization, consistent with the literature, which shows that increased population pressure and land conversion contribute to UHI formation (He et al., 2025). The spatial spread indicates a decline in natural cooling surfaces and an increase in built-up density.

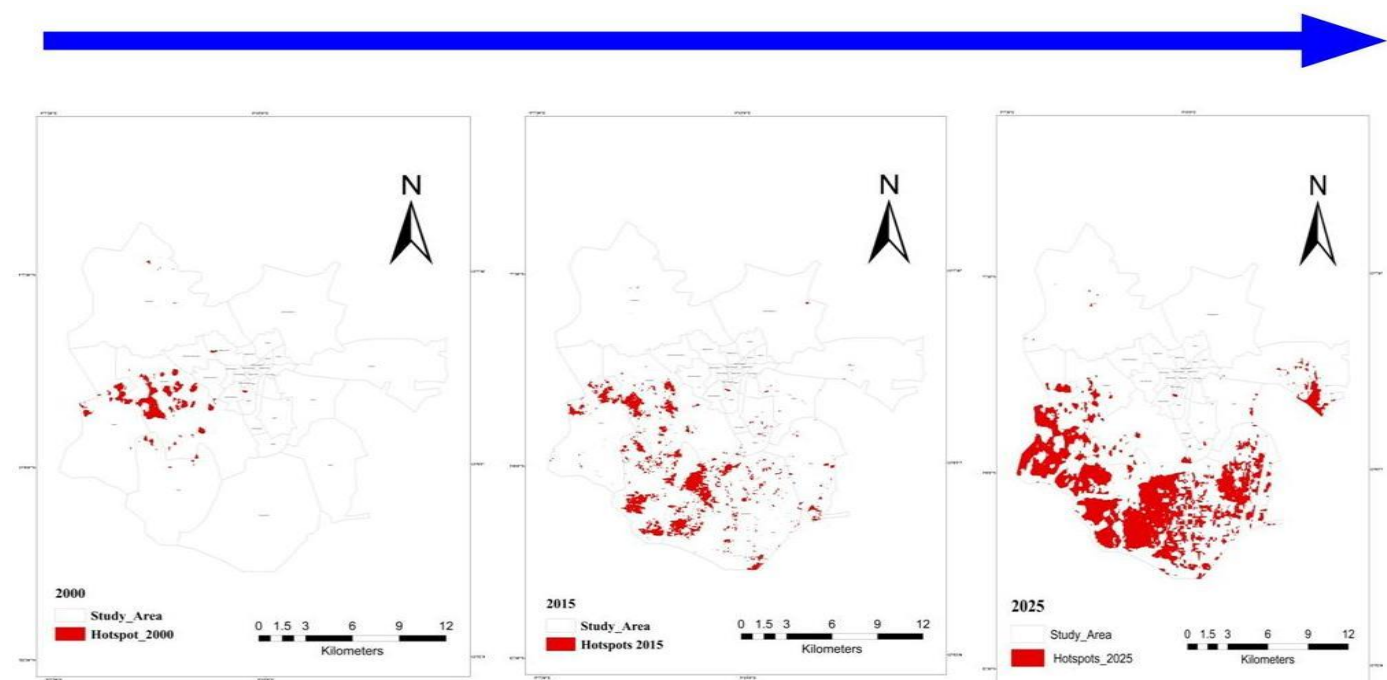


Figure 5: UHI Hotspots 2000, 2015, and 2025

The 2025 map shows very large, dense, and continuous hotspots, forming major hotspot belts across the southern, southwestern, and southeastern zones. These areas represent the most urbanized sections of Sokoto Metropolis. The strong clustering of hotspots indicates severe UHI intensity, typical of cities with highly compact development and minimal vegetation (Rahman et al., 2023). The transition from isolated hotspots (2000) to continuous belts (2025) reflects the city's rapid urban growth and near-complete conversion of green spaces into built-up areas. The analysis of the NDVI maps for 2000, 2015, and 2025 indicates a consistent decline in vegetation cover across Sokoto Metropolis. Vegetated areas decreased from approximately 42% in 2000 to 32% in 2015 and further to approximately 20% in 2025. Overall, vegetation declined by more than half ($\approx 52\%$) between 2000 and 2025 (over 25 years). The loss is most

pronounced in the central urban area, where built-up expansion has replaced natural vegetation. The most affected areas are the central metropolis (near-complete vegetation disappearance due to urban densification), northern corridor (formerly continuous vegetation now broken into isolated patches), southern zones (agricultural vegetation replaced with settlements), and eastern areas (still vegetated but reduced in density).

3.5 Relationship between Green Space Loss and UHI Intensity

The results revealed a significant positive correlation between the impervious surface area and UHI intensity, indicating that urban expansion and green space loss contribute to increased UHI effects, and those built-up areas tend to experience higher temperatures. Conversely, a strong negative correlation was observed between the NDVI and LST, indicating that green spaces tend to mitigate UHI effects (see Table 3).

**Table 3: Relationships between UHI intensity and vegetation cover**

Year	Vegetation (NDVI)	LST Pattern	Interpretation
2000	High vegetation cover	Lower to moderate LST	Vegetation helps cool surfaces through evapotranspiration
2015	Vegetation decreased	High LST dominates	Less vegetation with higher heat retention
2025	Very low vegetation	Mostly high LST	Urban heat island intensifies; reduced cooling effect

The combined analysis of the NDVI and LST for 2000, 2015, and 2025 revealed a strong inverse (negative) relationship between vegetation cover and land surface temperature across the Sokoto metropolis. This means that areas with high vegetation cover have lower temperatures, whereas areas with reduced vegetation cover have significantly higher temperatures. The spatial patterns in both datasets reinforce this relationship. In 2000, the high-vegetation to low-temperature NDVI map indicated moderate to high vegetation in the northern, northeastern, and parts of the central zones. Correspondingly, the LST map shows low to moderate temperatures in these same zones.

Areas with low NDVI values (south, southwest, and west) align with higher LST values, indicating the early formation of heat-prone surfaces. Vegetation still provided cooling effects, reducing surface temperatures in the greener zones. In 2015, the decrease in vegetation due to temperature increased the decrease in the NDVI noticeably across the metropolis; vegetated areas shrank into small pockets, mostly in the northern and a few peri-urban zones. LST maps reveal a significant increase in high-temperature areas, especially in the central metropolis, western corridor, and southern expansion zones. As vegetation declined, the LST values increased in the same areas.

The reduction in green cover corresponds to the expansion of built-up and bare soil areas, both of which

absorb and reradiate heat more intensively. Zones with substantial green space loss consistently align with higher LST values (Gandu, Tuntube-Tsefe, Kalambaina, and Tudun-Wada), indicating spatial coupling between depletion and heat intensity. The analysed Landsat images from 2000, 2015, and 2025 indicated that the NDVI and LST have indirect relationships.

3.6 Correlation Trend (2000–2025)

Across the 25 years, three consistent patterns emerged. These are:

- Vegetation decreases with increasing temperature (see Table 4). As the NDVI values declined from moderate/high in 2000 to very low in 2025, the LST increased from mixed moderate/high in 2000 to predominantly high in 2025.
- Spatial alignment strengthens the inverse relationship. Areas with persistently low NDVI values (south, west) remained hotspots throughout. The former green areas (north, northeast) transitioned from low LST (2000) to high LST (2025) as vegetation was lost.
- Urban expansion intensifies heat intensity. The urban growth patterns overlap with the decrease in the NDVI, reinforcing the urban heat island (UHI) effect.

Table 4: Comparison of mean and standard deviation of NDVI and LST values

Year	Mean NDVI	NDVI SD	Mean LST (°C)	LST SD (°C)	Interpretation
2000	0.14	0.06	38	1.6	Moderate vegetation cover corresponds to lower and more variable LST values.
2015	0.13	0.04	43	2.5	Noticeable vegetation decline results in higher temperatures across most areas.
2025	-0.24	0.4	45	3.2	Very low NDVI corresponds to widespread high LST, confirming a strong negative correlation

4 Discussions

Overall, the temporal analysis from 2000 to 2025 revealed a progressive increase in land surface temperature accompanied by a decrease in vegetation cover within Sokoto Metropolis (Gandu, Tuntube-Tsefe, Kalambaina, and Tudun-Wada). These findings confirm that vegetation loss is a key driver of temperature variation and urban heat island formation. The interaction between the NDVI and LST across Sokoto Metropolis from 2000–2025 reveals a strong inverse relationship, and decreasing vegetation cover is directly associated with increasing surface temperatures. This finding is in congruence with that of Abubakar et al. (2024), who also established a strong negative relationship ($r = -0.704$) between vegetation loss and daytime LST in Kaduna Metropolis from 2003 to 2023. A study by Ogunjobi et al. (2018) revealed that urban areas are relatively devoid of vegetation, especially trees that provide shade and cool the air through evapotranspiration, which has been altered by the built-up environment. UHIs are spatially clustered and concentrated in rapidly urbanized wards.

The few, isolated, and small hotspots, concentrated mainly in the south-western portions of the metropolis, shown by the 2000 hotspot map, correspond with most other areas that displayed low thermal clustering. This suggests early-stage urban development and minimal UHI formation, a scenario vividly reported by Dangulla et al. (2024). Low hotspot intensity is typical of cities with significant natural land cover and low population density, as observed by Kong et al. (2021). A large portion of hotspot pixels spatially coincided with areas where green cover was removed between 2000 and 2025, suggesting a spatial association between green space depletion and elevated LST. By 2015, hotspots became more numerous and spatially dispersed, extending into central and southern regions. Patches were larger and more fragmented than in 2000. This reflects accelerated urbanization, consistent with the literature, which shows that increased population pressure and land conversion contribute to UHI formation (He et al., 2025). The spatial

spread indicates a decline in natural cooling surfaces and an increase in built-up density. A low NDVI value corresponds to a high LST, and high NDVI values correspond to a low LST. Generally, a negative correlation was found between the NDVI values and the LST. This finding is in agreement with those of many scholars (Abubakar et al., 2024; Ogunjobi et al., 2018; Feyisa et al., 2014).

5 Conclusion

The study identified and mapped UHI hotspots in Sokoto Metropolis, revealing a significant relationship between green space depletion and UHI intensity. Land surface temperature (LST) mapping revealed clear spatial clusters of elevated LSTs (UHI hotspots) concentrated in heavily built and impervious zones of Sokoto Metropolis. The study concludes that areas with the most pronounced green space depletion (dense residential expansion) coincided with the highest LST values and the broadest UHI intensity. Green patches (parks, riparian strips, and institutional vegetated areas) presented consistently lower LST values and acted as local temperature depressors (cool islands) within the urban fabric. The produced maps (LST maps, normalized difference vegetation index (NDVI) maps, and hotspot overlay maps) demonstrate spatially explicit relationships between vegetation loss and UHI occurrence and intensity. Hotspot persistence analysis suggests that some UHI zones are long-standing (driven by entrenched land use and low vegetation), whereas others are emergent (recent development or degradation). In view of the foregoing, this study recommends embarking on robust re-greening efforts and safeguarding of green spaces in Sokoto metropolis to mitigate the UHI effect, and that authorities should make use of the generated hotspot maps to guide zoning decisions, discourage high-intensity development in currently vulnerable residential areas, and prioritize greening or shading interventions where people are most exposed.

References

Abdelnour, M. and Engel, B. (2018). Application of remote sensing techniques and geographic information systems to analyze land surface temperature in response to land use/land cover change in the Greater Cairo Region, Egypt. *J. Geogr. Inf. Syst.* 10 (2018) 57–88. <https://doi.org/10.4236/jgis.2018.101003>

Abubakar, M. L., Thomas, D., Ahmed, M. S., & Abdussalam, A. F. (2024). Assessment of the Relationship Between Land Surface Temperature and Vegetation Using MODIS NDVI and LST Timeseries Data in Kaduna Metropolis, Nigeria. *FUDMA Journal of Sciences*, 8(2), 137–148. <https://doi.org/10.33003/fjs-2024-0802-2305>

Adamu, I. A., Murtala, D. and Eniolorunda, N.B. (2015): Human Impact and the Degradation of Biodiversity Resources – A case Study of Some Vegetation Patches in Sokoto Metropolis, Sokoto State, Nigeria (1999-2014) – A paper presented at the Annual Conference of the Association of Nigerian Geographers held at Osun State University, Osogbo, 24-25, February, 2015 https://www.researchgate.net/publication/330701314_An_inventory_of_biodiversity_resources_in_some_vegetation_patches_in_Sokoto_Metropolis_Sokoto_State

Adamu, I. A., and Umar, A. (2015): Greenbelt Conversion, Climate Change and the Declining Quality of Environment in Urban Sokoto, Nigeria (1998-2015) – A Sustainable Development Perspective book chapter contributed to Security, National Integration and the Challenges of Development in Nigeria publication of the Faculty of Social Sciences, Usmanu Danfodio University Sokoto.

Adegun, O. B., Ayodele Ikudayisi, E. Morakinyo, T.E., and Olusoga,



O.O. (2021). Urban Green Infrastructure in Nigeria: A Review, *Scientific African*. <https://doi.org/10.1016/j.sciaf.2021.e01044>

Dangulla, M., Abd Manaf, L., and Ramli, M. F. (2024). Determining The Response Of Vegetation To Urbanization And Urban Expansion In Sokoto Metropolis, Sokoto State, Nigeria *Journal of Research in Forestry, Wildlife & Environment* 16(4) 186-207 <http://www.ajol.info/index.php/jrfwe>

Dantuni, D. (2011). Appraisal of the Implementation of Sokoto Master Plan 1983 – 2003. Unpublished Dissertation, Danfodiyo University, Sokoto, Nigeria

Eniolorunda, N. B. (2010). Assessment of Vegetation Degradation in Sokoto Northeast: A Remote Sensing Approach. *Environmental Issues*, 3(1), 64-73.

Eniolorunda, N. B. and Dankani, I. M. (2020). Assessment of Urban growth pattern in Sokoto Metropolis, Nigeria, using multitemporal satellite data. *Nigeria Geographical Journal*, Volume 8(1) June 2012

Feyisa, G. L.; Dons, K.; Meilby, H (2014). Efficiency of parks in mitigating urban heat island effect: An example from Addis Ababa. *Landscape and Urban Planning* 123, 87-95. <https://doi.org/10.1016/j.landurbplan.2013.12.008>

Hadjimitsis, D. and Themistocleous, K. (2008). The importance of considering atmospheric correction in the pre-processing of satellite remote sensing data is intended for the management and detection of cultural sites: a case study of the Cyprus area, in: *Digital Heritage* in: M. Ioannides, A. Addison, A. Georgopoulos, L. Kalisperis, (eds)- Proceedings of the 14th International Conference on Virtual Systems and Multimedia.

He, P., Chen, Z., Zhang, L., Ma, C., & Luo, C. (2025). Machine learning prediction of future land surface temperature from SAR optical fusion under urban expansion in Changsha, China. *Scientific Reports*. <https://doi.org/10.1038/s41598-025-30976-5>

Kong, J., Zhao, Y., Carmeliet, J., & Lei, C. (2020). Urban Heat Island and Its Interaction with Heatwaves: A Review of Studies on Mesoscale. *Sustainability*, 13(19), 10923. <https://doi.org/10.3390/su131910923>

Mensah, C. A. (2014) Urban Green Spaces in Africa: Nature and Challenges *International Journal of Ecosystem* 2014, 4(1): 1-11 <https://doi.org/10.5923/j.ije.20140401.01>

Martinová, V., Gallay, I., & Olah, B. (2022). Mitigating the Effect of Urban Green Spaces on Surface Urban Heat Island during Summer Period in the Example of a Medium Size Town of Zvolen, Slovakia. *Remote Sensing*, 14(18), 4492. <https://doi.org/10.3390/rs14184492>

National Population Commission (NPC, 2007). Population Census Data, Nigeria, Federal Republic of Nigeria Official Gazette, National and State Provisional Total Census, Printed and Published in Federal Government Printer, Lagos, No 21-vol.94,

Ogunjobi, K. O., Adamu Y., Akinsanola, A. A., and Orimoloye, I. R. (2018). Spatiotemporal analysis of land use dynamics and its potential indications on land surface temperature in Sokoto Metropolis, Nigeria. *R. Soc. open sci.* 5: 180661. <http://dx.doi.org/10.1098/rsos.180661>

Rahman, M. N., Rony, M. R. H., Jannat, F. A., Chandra Pal, S., Islam, M. S., Alam, E., & Islam, A. R. M. T. (2022). Impact of Urbanization on Urban Heat Island Intensity in Major Districts of Bangladesh Using Remote Sensing and Geo-Spatial Tools. *Climate*, 10(1), 3. <https://doi.org/10.3390/cli10010003>

Umar, A., Adamu, I.A., & Yelwa, S. A. (2018): Ecological Faults and Offences in Buildings and Urban Designs of Sokoto Metropolis, Northwestern Nigeria and their Implications for Individuals' Coping with Thermal Discomfort *Nigerian Journal of Renewable Energy* 18, (1&2): 214-222 https://www.researchgate.net/publication/398677000_ecological_faults_and_offences_in_buildings_and_urban_designs_of_sokoto_metropolis_northwestern_nigeria_and_their_implications_for_individuals'_coping_with_thermal_discomfort

Umar, A. T. (2013). Evidence of Climate change. In Iliya M. A. and Fada A. G. (eds.). *The impact of climate change on Sokoto State, Nigeria: Evidence and Challenges*, 1st edition, UNDP/Sokoto State Government

Yan, J., Yin, C., An, Z., Mu, B., Wen, Q., Li, Y., Zhang, Y., Chen, W., Wang, L., and Song, Y. (2023). The Influence of Urban Form on Land Surface Temperature: A Comprehensive Investigation from 2D Urban Land Use and 3D Buildings, *Land* 12(9), 1802. <https://doi.org/10.3390/land12091802>

Yelwa, S. A., Eniolorunda N. B., and M. M. Badamasi (2009): Application of Remote Sensing and GIS to Agricultural Land Encroachment: A case Study of Sokoto-Rima Valley, Sokoto. *Journal of Agriculture and Environment*, Vol. 5 (1&2), pp. 97-107,

Zhou, D., Zheng, Y., & Li, J. (2017). The urban heat island effect and its relationship with urbanization in China: A review. *Atmosphere*, 8(6), 96. <https://doi.org/10.3390/atmos8060096>